

Investigation of Solid-State Reactions Using Variable Temperature X-Ray Powder Diffractometry. II. Aminophylline Monohydrate

Suneel K. Rastogi,^{1,2} Marek Zakrzewski,^{3,4} and Raj Suryanarayanan^{1,5}

Received May 22, 2002; Accepted May 30, 2002

Purpose. The object of this investigation was to demonstrate the utility of X-ray powder diffractometry (XRD) to study the kinetics of a complex pharmaceutical solid-state reaction wherein the reactant, product and intermediate phases were all simultaneously quantified.

Methods. Aminophylline monohydrate (**I**) decomposed to anhydrous theophylline (**III**) either directly or through an intermediate (anhydrous aminophylline, **II**). The reaction kinetics were studied isothermally at several temperatures ranging from 65 to 100°C. By measuring the intensities of the XRD peaks unique to **I**, **II** and **III**, it was possible to simultaneously quantify the 3 phases during the entire reaction.

Results. Assuming that all the reaction steps follow first-order kinetics, the three equations describing the concentrations of **I**, **II** and **III** as a function of time, were derived. By fitting the experimental data to these equations, it was possible to obtain the rate constants for the three reaction steps. The rate constants were obtained at different temperatures and were used to draw Arrhenius type plots from which the activation energies were determined. At lower temperatures (<80°C), the concentration of the intermediate phase, i.e., **II**, was low throughout the reaction while at higher temperatures (>90°C), there was rapid formation and accumulation of **II** during the early stages of the reaction. These differences could be attributed to the fact that k_1 (**I** → **II**) had a more pronounced temperature dependence than k_2 (**I** → **III**) and k_3 (**II** → **III**). The XRD results were confirmed with isothermal thermogravimetry.

Conclusions. Variable temperature XRD is a powerful tool to probe reaction kinetics in crystalline pharmaceuticals since it permits simultaneous quantification of multiple solid phases.

KEY WORDS: kinetics; solid-state; theophylline; aminophylline; decomposition; X-ray powder diffractometry.

INTRODUCTION

The active ingredient and the excipients in a solid dosage form can undergo chemical decomposition as well as physical transformation reactions. Physical transformations include polymorphic transitions, changes in state and degree of solvation and alterations in degree of crystallinity. Some types of chemical reactions in solid pharmaceuticals are oxidation, hydrolysis and photochemical reactions (1–8). These changes

can be induced during pharmaceutical processing and/or storage and can profoundly influence the performance as well as the shelf-life of dosage forms. The kinetics and mechanism of solid-state reactions are influenced by several factors including temperature, water vapor pressure, and processing.

Differential scanning calorimetry and thermogravimetry have been extensively used to study solid-state decomposition kinetics. However, these techniques have several drawbacks. For example, they do not unambiguously identify crystalline phases (if any) and are not necessarily useful for discerning the reaction mechanism (9). These drawbacks can be overcome by using the technique of X-ray powder diffractometry (XRD). Since the diffraction pattern of each crystalline form of a compound is unique, XRD is particularly suited for the analyses of solid mixtures. Moreover, the intensities of the peaks unique to each phase enable quantitative analyses (10,11). Thus, simultaneous quantification of crystalline reactants, products and intermediates (if any) are possible. If an amorphous intermediate is formed, this usually becomes evident from mass balance calculations (12). Thus the technique is ideally suited to understand reaction mechanisms.

Several advances in XRD instrumentation and software have greatly facilitated the study of pharmaceutical systems. Variable temperature XRD is a technique where XRD patterns are obtained while a sample is subjected to a controlled temperature program. The kinetics of dehydration, racemization and crystallization reactions have been studied by this technique (12–14). While the dehydration of theophylline monohydrate has been the subject of numerous investigations, only variable temperature XRD revealed the formation of a metastable anhydrate, which then transformed into the stable anhydrate (5). Recently, it has also become possible to control the water vapor pressure in the XRD sample chamber (9,15–17). Another advancement in instrumentation is the position sensitive detector (PSD) which enables very rapid data collection. Finally, reliable data analyses programs have become available, which are particularly useful to decompose asymmetric and overlapping X-ray peaks.

In an earlier investigation, we had demonstrated the utility of variable temperature XRD in the study of simple, one-step decomposition and phase transformation reactions (18). In this project, we have extended the utility of XRD to study more complex solid-state reactions. Theophylline, a bronchodilator effective in the treatment of asthma, is only slightly soluble in water. Complexation of theophylline with ethylenediamine to form aminophylline considerably enhances the aqueous solubility. The decomposition of aminophylline was investigated since an understanding of the reaction kinetics and mechanism may facilitate the preparation of stable aminophylline formulations.

Several solid forms of aminophylline have been reported in the literature including an anhydrate (19), a hemihydrate (20), a monohydrate (20,21), a dihydrate (19) and a hepta hemihydrate (20). The solid-state decomposition of the monohydrate has been investigated using thermogravimetry (21,22). Ishiguro *et al.* (22) found that the elimination of ethylenediamine from aminophylline was a first-order process. Nishigo *et al.* (21) showed that the decomposition of **I** is a complex process involving three elementary steps as shown later (Scheme 1). Our studies revealed that the intermediate

¹ College of Pharmacy, 308 Harvard St. S.E., University of Minnesota, Minneapolis, Minnesota 55455.

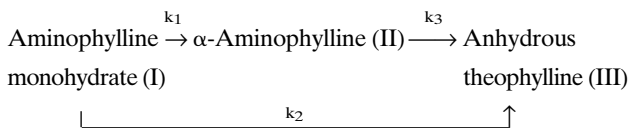
² Present address: Forest Laboratories, Inc., 330 Prospect Street, Inwood, New York 11096.

³ Philips Analytical X-ray, Almelo, The Netherlands.

⁴ Present address: Advanced Solid State Analysis International, Inc., 3B East Lake Road, Danbury, Connecticut 06811.

⁵ To whom correspondence should be addressed. (e-mail: surya001@umn.edu)

(α -aminophylline; **II**) was aminophylline anhydrate. The structures of anhydrous aminophylline and its decomposition product theophylline are given in Fig. 1.



Scheme 1. Solid-state decomposition of aminophylline monohydrate (**I**) wherein k_1 , k_2 and k_3 are the rate constants for the elementary steps. All three phases, **I**, **II** and **III**, are highly crystalline.

This complex decomposition reaction offers several analytical challenges. In addition to the formation of an intermediate (**II**), the same product (**III**) is obtained through two pathways. Conventional thermoanalytical techniques (DSC, TGA) yield complex profiles due to overlapping thermal events. As a result it is not possible to separate the reaction steps and study them individually. Since XRD permits simultaneous quantification of the reactant, intermediate and product, mass balance calculations are possible at all stages of the reaction. It is not only possible to separate the reaction steps, the rate constant and activation energies of each step can also be independently determined.

Therefore, the overall goal of this project was to establish the utility of XRD to study complex multi-step solid-state decomposition reactions. The specific objectives were the following: (i) to study the decomposition kinetics of aminophylline monohydrate by simultaneously quantifying the reactant, intermediate and product phases and obtain the values of k_1 , k_2 and k_3 (Scheme 1); (ii) to determine the effect of tempera-

ture on the kinetics of each reaction step, i.e. the effect of temperature on the magnitudes of k_1 , k_2 and k_3 ; (iii) to compare the results obtained by XRD with that obtained by thermogravimetric analysis.

MATERIALS AND METHODS

Aminophylline monohydrate (**I**; Sigma), ethylenediamine (Sigma), anhydrous theophylline (Sigma), and absolute alcohol (200 Proof; Aaper Alcohol and Chemical) were used as received.

Preparation of Anhydrous Aminophylline (II)

Anhydrous theophylline (19.8 g) was dispersed in 50 ml solution (10% v/v) of ethylenediamine in absolute alcohol. This was stirred continuously at room temperature for 4 h. The precipitate was filtered and washed thoroughly with absolute alcohol and dried at room temperature under vacuum for 12 h.

Thermal Analysis

A differential scanning calorimeter (DSC, model 910, TA Instruments) and a thermogravimetric analyzer (TGA, model 951, TA Instruments) were connected to a data analysis system (Thermal analyst 2000, TA Instruments). The DSC was calibrated with indium. Both open pans and non-hermetically crimped pans were used. About 4–7 mg of **I** was weighed into an aluminum pan and heated, under a stream of nitrogen, from 25 to 200°C at 10°C/min. For the isothermal thermogravimetric analysis, about 4–7 mg of **I** was weighed into an open aluminum pan and maintained isothermally at the desired temperature. These studies were conducted at 70, 85 and at 100°C.

Karl Fischer Titrimetry

The water content was determined using a Karl Fischer titrimer (Model CA-05 Moisture Meter, Mitsubishi).

Hot Stage Microscopy

The sample was dispersed on a slide, a drop of silicon oil was added and then a cover slip was placed over it. It was heated at 10°C/min on a hot stage microscope (Mettler FP82HT) and observed continuously.

Reaction under Isothermal Conditions

The studies were carried out in a θ - θ X-ray powder diffractometer (Philips X'Pert-MPD system) with a non-ambient attachment (model TTK, Anton Paar) and a position sensitive detector (RAYTECH®) in the static mode. Since the sample stage is held in a fixed position in a θ - θ diffractometer, it is ideally suited to monitor solid-state reactions. The sample stage was aligned using an alignment tool made up of a silicon crystal. The drug powder was filled into an X-ray holder, maintained isothermally at the desired temperature and subjected to XRD, at regular time intervals. The data collection time in the position sensitive detector ranged between 30 and 120 seconds with slower reaction rates permitting data collection over longer time periods. The experiments were repeated at several temperatures in the range of 65°C to 100°C. At the

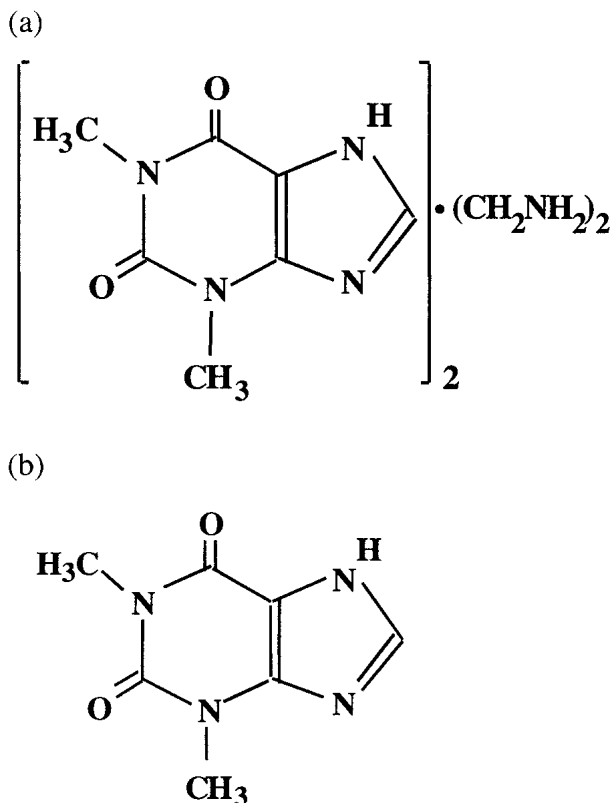


Fig. 1. Structures of (a) anhydrous aminophylline, and (b) theophylline.

end, in order to confirm that the reaction had gone to completion, the temperature was increased to 125°C, held for 2 min, and the XRD pattern was obtained. At this temperature, based on thermal analysis, rapid and complete transformation to **III** is expected. Moreover, there was complete disappearance of the XRD peaks unique to **I** and **II**. This was further evidence of completion of the reaction. Because of the high temperature range of the experiments, the atmosphere around the sample was dry. For all practical purposes, it can be assumed that the water vapor pressure around the sample was 0 Torr.

Selection of Temperature Range

TGA curve of **I** revealed overlapping weight loss steps indicating that the loss of water and ethylenediamine occurred simultaneously. Since the weight loss occurred between 60 and 130°C, this temperature range was initially selected for the isothermal XRD studies. However, at 60°C, the reaction proceeded very slowly. On the other hand, at temperatures $\geq 105^\circ\text{C}$, the reaction proceeded so rapidly that there was insufficient time for the measurement of peak intensities. Therefore, isothermal XRD experiments were conducted over the temperature range of 65 to 100°C.

Selection of Angular Range

Variable temperature XRD of **I** revealed that the peaks unique to **I** (at 10.8 and 11.9°2 θ), **II** (11.3°2 θ) and **III** (12.7°2 θ) did not significantly overlap with each other. Thus, the range of 10 to 13.5°2 θ was selected for monitoring the decomposition kinetics. The quantification of **I** was based on the sum of the integrated intensities of the peaks at 10.8 and 11.9°2 θ , while the intensities of the 11.3 and 12.7°2 θ peaks were used to quantify **II** and **III** respectively.

There were some complicating factors in the quantitative analyses. In reaction mixtures of **I**, **II** and **III**, there was some overlapping of peaks, during the intermediate stages. The peaks were decomposed using software provided by Philips (Philips Profit). The second problem was due to asymmetric peak profiles. Using pure phases of **I**, **II** and **III**, the profile fitting of the individual peaks of interest was accomplished. These parameters were used during peak decomposition. Thus the software enabled the determination of the areas of asymmetric and overlapping peaks. Appropriate background subtraction was also performed using this software (23).

RESULTS AND DISCUSSION

Characterization of Aminophylline Monohydrate (**I**)

The XRD pattern of **I** (Fig. 2) matched with that of aminophylline monohydrate reported in the literature (20,21). The water content of 4.0% w/w was identical to the stoichiometric water content in the monohydrate, strongly suggesting the absence of sorbed water. When the sample was dispersed in silicon oil and subjected to hot stage microscopy, bubbles emanated between 115 and 118°C and then again at ~150°C, suggesting a gaseous reaction product. The DSC and TGA profiles depended on the type of pan used (Fig. 3). When **I** was subjected to DSC in open pans (Fig. 3a), a broad endotherm was observed over the temperature range of 60°C to 130°C (21). In this temperature range, TGA revealed a

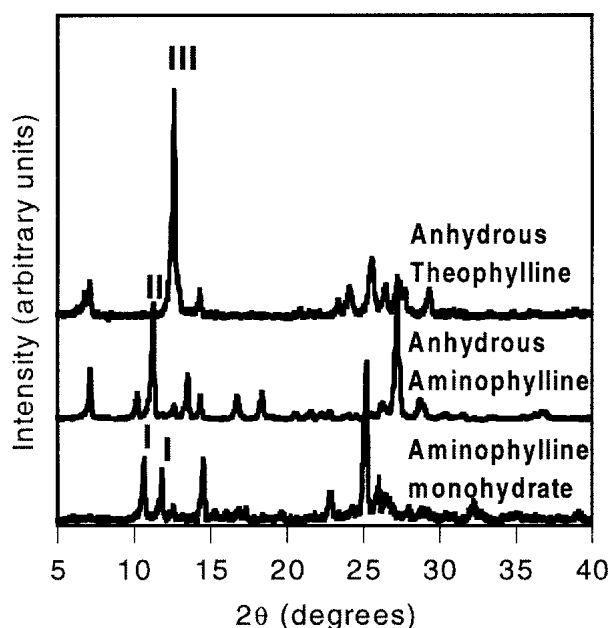


Fig. 2. XRD patterns of aminophylline monohydrate (**I**), anhydrous aminophylline (**II**) and anhydrous theophylline (**III**). The peaks unique to each phase are indicated.

weight loss of ~17%. This was close to the calculated weight loss of 17.8% for the complete removal of lattice water in the monohydrate as well as ethylenediamine. **I** therefore appears to lose both water and ethylenediamine to form anhydrous theophylline. This was confirmed by variable temperature XRD of **I**. The powder pattern at 150°C matched with that of stable anhydrous theophylline (**III**) (24). This indicates complete conversion of **I** to **III**. The XRD pattern of **III** is presented in Fig. 2.

When **I** was heated in nonhermetically crimped pans, endotherms at ~119°C and 150°C were observed (Fig. 3b). In order to determine if the first thermal event was readily reversible, the sample was heated up to 125°C in the DSC, allowed to cool back to room temperature and immediately reheated to 170°C. Since no thermal event was observed up to ~125°C, the first endotherm cannot be attributed to a readily reversible process such as an enantiotropic polymorphic transition. The second endotherm was observed though the peak was slightly broadened. When the sample was cooled to room temperature and again heated to 180°C, no thermal event was observed. Therefore, the second endotherm is also unlikely to be due to a readily reversible process.

Based on these observations, we can postulate that the first endotherm is due to dehydration accompanied by vaporization of water and the second endotherm is due to the loss of ethylenediamine. KFT of the sample heated in the DSC to 125°C revealed negligible water content. Next, **I** was heated in the DSC up to 125°C, cooled to room temperature and stored at 24°C/75%RH for 2 days and again subjected to DSC. The DSC curve was similar to that of "as is" **I**, with the reappearance of the endotherm at 117°C followed by a second endotherm at 147°C. Therefore, the first endotherm could be attributed to water loss. Its reappearance following storage is due to rehydration at high water vapor pressure (75% RH). However, in the stored sample, the enthalpy values of both these transitions were significantly lower than that of the "as

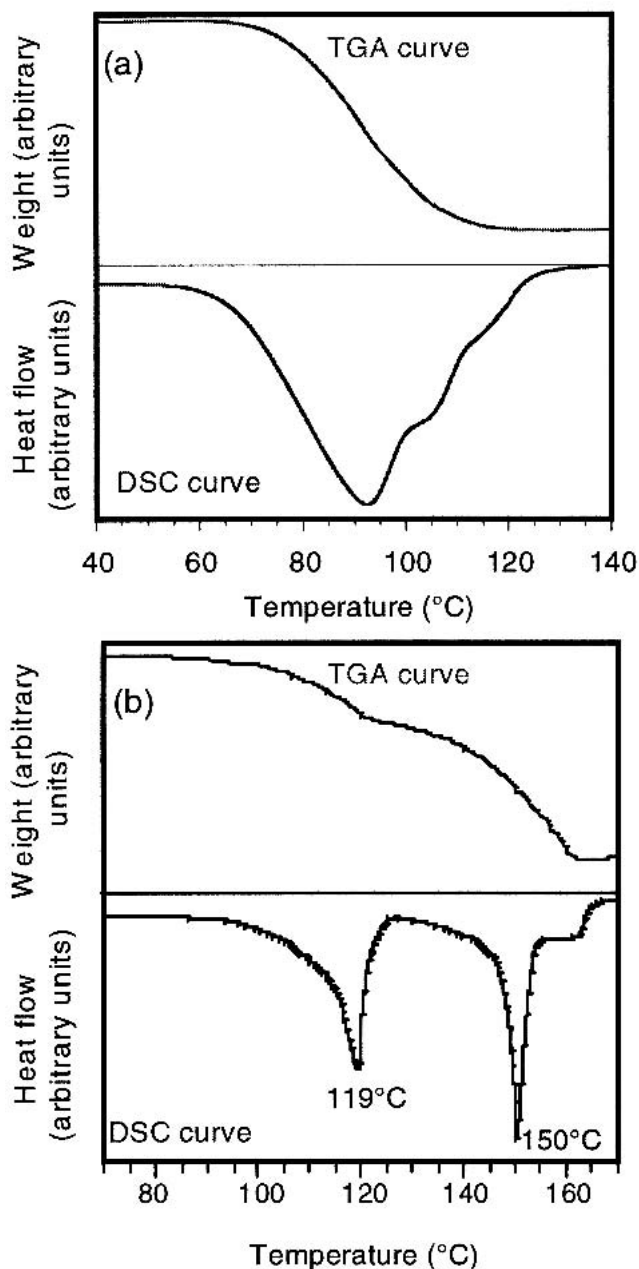


Fig. 3. DSC and TGA curves of aminophylline monohydrate (**I**) obtained using (a) open pans and (b) non-hermetically crimped pans.

is" sample. Therefore, we postulate that there are two thermal events during the first endotherm—complete loss of water and partial loss of ethylenediamine to form a mixture of anhydrous aminophylline and anhydrous theophylline. When stored at 24°C/75% RH, only the dehydrated aminophylline gets rehydrated while theophylline cannot be converted to aminophylline. Our postulate is supported by the observation that the enthalpy ratio of the second endotherm to the first endotherm in the stored sample is the same as in the "as is" sample. Therefore, when **I** was heated in a crimped pan, the first endotherm was due to complete dehydration and partial loss of ethylenediamine, followed by a second endotherm due to the loss of the remaining ethylenediamine.

Characterization of the Prepared Aminophylline Anhydrate (**II**)

The XRD pattern of the sample (Fig. 2) was similar to that of α -aminophylline reported in the literature (21). Karl Fischer titrimetry revealed negligible water content proving that the sample was an anhydrate. TGA indicated a weight loss of ~14.30%, which is close to the stoichiometric ethylenediamine content of 14.28% in the anhydrate.

Theoretical Basis of Quantitative X-Ray Diffractometric Analyses

Klug and Alexander (23) derived the expressions for the quantitative analysis of crystalline components in powder mixtures. A solid mixture consisting of several components can be regarded as consisting of only two components—the analyte (component "a") and the sum of the other components designated as the matrix (component "M"). The relationship between the intensity of a characteristic line of analyte "a", I_a , and its weight fraction x_a is given by Eq. (1).

$$\frac{I_a}{(I_a)_0} = \frac{x_a \mu_a^*}{x_a(\mu_a^* - \mu_M^*) + \mu_M^*} \quad (1)$$

Here $(I_a)_0$ is the intensity of the same line in a sample consisting of only analyte "a," and μ_a^* & μ_M^* are the mass attenuation coefficients of "a" (analyte) and "M" (matrix) respectively. When **I** is considered the analyte, the matrix consists of **II** and **III**. Similarly when **II** or **III** is considered the analyte, the matrix consists of (**I** and **III**) and (**I** and **II**) respectively.

The mass attenuation coefficient of a compound is the weighted average of the mass attenuation coefficients of its constituent elements. The mass attenuation coefficients of **I**, **II** and **III** were calculated to be 6.53, 6.38 and 6.55 cm^2g^{-1} (CuK α radiation) respectively. Since these values were close to one another, it was assumed that the mass attenuation coefficients of **I**, **II** and **III** were the same (i.e., $\mu^*_I \equiv \mu^*_{II} \equiv \mu^*_{III}$). Eq. (1) then simplifies to

$$\frac{I_a}{(I_a)_0} = x_a \quad (2)$$

Thus, during the kinetic study, the weight fraction of the analyte (x_a) can be obtained from the intensity of line unique to the analyte (I_a) at any time t , and the intensity of the same line in a sample consisting only of the analyte, $(I_a)_0$.

Decomposition Kinetics

Figure 4 contains the XRD patterns of aminophylline monohydrate (**I**) maintained isothermally at 75°C. The formation of the intermediate, aminophylline anhydrate (**II**) and theophylline (**III**) is strongly suggested by the peaks unique to each of these phases. In another experiment, in order to confirm the formation of aminophylline anhydrate (**II**), **I** was maintained at 80°C and XRD patterns were obtained at regular time intervals. After 125 min, all the peaks unique to **I** had disappeared, indicating that the decomposition of **I** was complete. At this time point, all the observed peaks could be attributed either to **II** or to **III**. Karl Fischer titrimetry of the sample cooled to room temperature revealed negligible water content. Based on these results, we concluded that the inter-

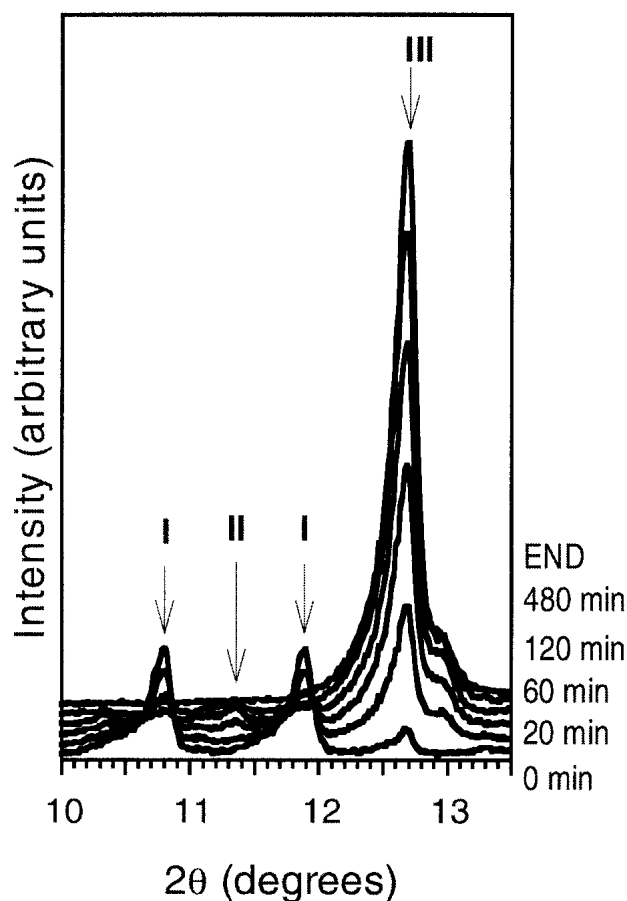


Fig. 4. Isothermal X-ray powder diffractometry of aminophylline monohydrate (**I**) at 75°C. XRD patterns were obtained at the time points indicated in the figure. The arrows point to peaks unique to **I**, **II** and **III**.

mediate phase was aminophylline anhydrate (**II**). Under all the experimental conditions, the reaction products were highly crystalline and there was no evidence for the formation of any amorphous intermediates.

The integrated intensities of these peaks were determined from powder patterns collected at different times. In order to calculate the weight fractions of **I**, **II** and **III** as a function of time (using Eq. 2), it was also necessary to experimentally obtain the appropriate $(I_a)_0$ values by subjecting pure **I**, **II** and **III** to XRD. The initial XRD pattern (i.e. pattern at time zero) yielded $(I_a)_0$ for **I**. **I** was completely converted to **III** by heating to 125°C and holding for 2 min. This yielded $(I_a)_0$ for **III**. This conversion was confirmed by both thermal analyses (Fig. 3a) and by XRD. It was not possible to directly obtain the $(I_a)_0$ value for **II**, because the XRD holder does not contain pure **II** at any point during the reaction. Therefore the $(I_a)_0$ value for **II** was calculated assuming that **I**, **II** and **III** are crystalline during the entire reaction.

$$x_I + x_{II} + x_{III} = 1 \quad (3)$$

Here x_I , x_{II} and x_{III} are the weight fractions of **I**, **II** and **III** respectively. Since x_I and x_{III} can be determined at each time point, x_{II} can be calculated from Eq. (3). The value of x_{II} and the experimentally determined I_a for **II** enabled us to calculate $(I_a)_0$ for **II** (using Eq. 2). It was possible to calculate $(I_a)_0$ of **II** at all time points of the reaction. For example, in the

experiment carried out at 95°C, the $(I_a)_0$ value was $33,314 \pm 1,352$ counts (Mean \pm SD; $n = 12$). The low coefficient of variation value of 4%, strongly suggests that amorphous intermediates are not formed during the reaction. This was also confirmed by the absence of amorphous halos and the approximately constant background counts during the entire reaction.

In order to obtain the value of the rate constants k_1 , k_2 and k_3 , a kinetic model was proposed where the three decomposition steps of aminophylline were assumed to be first-order processes. Carstensen had provided the theoretical basis for the approximate first-order decomposition reaction in pharmaceuticals and there are numerous examples in the literature of solid-state decomposition reactions following this rate law (13,25,26). The change in the mole fractions of **I**, **II** and **III** as a function of time are described by Eqs. 4, 5 and 6 respectively.

$$\frac{d(\alpha_I)}{dt} = -(k_1 + k_2)\alpha_I \quad (4)$$

$$\frac{d(\alpha_{II})}{dt} = k_1\alpha_I - k_3\alpha_{II} \quad (5)$$

$$\frac{d(\alpha_{III})}{dt} = k_2\alpha_I + k_3\alpha_{II} \quad (6)$$

α_I , α_{II} and α_{III} refer to the mole fractions (the ratio of number of moles at time "t" to that if the holder was filled with the pure phase) of **I**, **II** and **III** respectively and k_1 , k_2 and k_3 were described previously (Scheme 1). Now, $\alpha_I = n_I/n_I^0$, where n_I is the number of moles of **I** at time "t" and n_I^0 is the initial number of moles of **I**; $\alpha_{II} = n_{II}/n_{II}^0$, where n_{II} is the number of moles of **II** at time "t" and n_{II}^0 is the number of moles if pure **II** is filled in the XRD holder; $\alpha_{III} = n_{III}/n_{III}^0$, where n_{III} is the number of moles of **III** at time "t" and n_{III}^0 is the final number of moles of **III**. The boundary conditions are: $\alpha_I = 1$ at $t = 0$ and $\alpha_I = 0$ at $t = \infty$; $\alpha_{II} = 0$ at $t = 0$ and $\alpha_{II} = 0$ at $t = \infty$; $\alpha_{III} = 0$ at $t = 0$ and $\alpha_{III} = 1$ at $t = \infty$.

The use of Eq. 2, experimentally provided the values of x_I , x_{II} and x_{III} . These were converted to α_I , α_{II} and α_{III} using the following relationship:

$$\alpha_i = \frac{x_i}{\sum_{i=I,II,III} \frac{x_i}{M_i}} \quad (7)$$

Here $i = \text{I, II or III}$ and M_I , M_{II} and M_{III} are the molecular weights of **I**, **II** and **III** respectively.

The differential equations (4) to (6) were solved and equations (8) to (10) are their respective integrated forms:

$$\alpha_I = e^{-(k_1+k_2)t} \quad (8)$$

$$\alpha_{II} = \left[\frac{k_1}{k_3 - k_1 - k_2} \right] [e^{-(k_1+k_2)t} - e^{-k_3t}] \quad (9)$$

$$\alpha_{III} = 1 - [e^{-(k_1+k_2)t}] - \left[\frac{k_1}{k_3 - k_1 - k_2} \right] [e^{-(k_1+k_2)t} - e^{-k_3t}] \quad (10)$$

These equations were solved in order to obtain the values of the rate constants k_1 , k_2 and k_3 . This was done as follows. Eq. (8) can be rewritten as:

$$\ln(\alpha_I) = -(k_1 + k_2)t \quad (11)$$

Thus, the plot of natural logarithm of α_I against time should result in a straight line passing through the origin. Figure 5 is such a plot obtained from the experimental data at 65 and 85°C. A linear relationship was also observed at all other temperatures (not shown). The slope of these plots gives the value of $(k_1 + k_2)$. The linear profiles also prove the validity of the assumption that the reaction steps **I** \rightarrow **II** and **I** \rightarrow **III** can be approximated to be first-order processes. The step **II** \rightarrow **III** was assumed to be first-order for the sake of simplicity. The assumption appears to be valid (discussed later).

Having obtained the value of $(k_1 + k_2)$, we next attempted to find the values of k_1 and k_3 using Eq. (10). The experimentally obtained values of α_{III} as a function of time were fitted to Eq. (10) by non-linear regression (Kaliedo-

graph® graphing software) using the known value of $(k_1 + k_2)$. This yielded the values of k_1 and k_3 . After $(k_1 + k_2)$ and k_1 are known, the value of k_2 could be calculated. In order to calculate the three rate constants, the concentrations as a function of time, of only two of the three phases are needed. The values of x_I and x_{III} were experimentally determined whereas x_{II} was obtained indirectly by the mass balance approach. Thus the values of α_I and α_{III} were deemed more reliable and were chosen for calculation of the rate constants.

The non-linear regression requires initial estimates of k_1 and k_3 . These were obtained from Equations (4) to (6) using research software (Stella®) which provides numerical solutions to simultaneous differential equations. The values of k_1 , k_2 and k_3 were refined until the best fit with the experimental data was obtained. These estimated values were then further refined using analytical solutions as described in the previous paragraph. The values of all the three rate constants obtained through the two methods were in good agreement.

From Equations (9) and (10), it is clear that the analytical solution is unsatisfactory when the value of k_3 is close to that of $(k_1 + k_2)$. In our study, we found that this was the case when the reaction was carried out at 65°C. In such a case the numerical solution obtained using Stella® software was used to plot the Arrhenius curves.

The experimentally obtained values of α_I , α_{II} and α_{III} as a function of time at 75°C and at 95°C were plotted (Fig. 6). The data points are experimental whereas the solid lines are generated from the rate constants using the proposed model (i.e. from Equations 8 to 10). There is a good agreement between the two. However, as seen in the figure, the model appears to overestimate α_{III} and underestimate α_{II} at later time points. This was particularly pronounced at the lower temperatures. This suggests that at later time points, a product layer is formed at the surface of the particles and the decomposition rate is limited by the diffusion of the gases (water vapor and ethylenediamine) through the product layer. Since the diffusion is slower at lower temperatures, the effect is more pronounced at lower temperatures. This is a very commonly observed feature in solid state thermal degradation reactions (27).

At higher temperatures, for example at 95°C (Fig. 6b), there was a sharp decrease in the concentration of **I**, until this phase became undetectable. This was accompanied by an increase in the concentrations of **II** and **III**. When the mole fraction of **II** (in the logarithmic scale) was plotted as a function of time (between 5 and 30 min), a linear profile was obtained (not shown). This strongly suggested that the transition of **II** \rightarrow **III** was also a first-order process.

The rate constant values obtained in the temperature range of 65 to 100°C were used to generate the Arrhenius plots (Fig. 7). From these linear plots, the activation energy values of the reactions: **I** \rightarrow **II**, **I** \rightarrow **III** and **II** \rightarrow **III** were calculated to be 220.1, 150.9, and 184.5 KJ/mole respectively. The temperature dependence of k_2 is the lowest while that of k_1 is the highest.

At higher temperatures (>90°C) there was an initial rapid increase in the concentration of **II**, following which its concentration gradually decreased until it could not be detected. At lower temperatures (<80°C), the concentration of **II** increased more gradually and it appeared to reach a steady-state. The disappearance of **II** was very gradual. These differ-

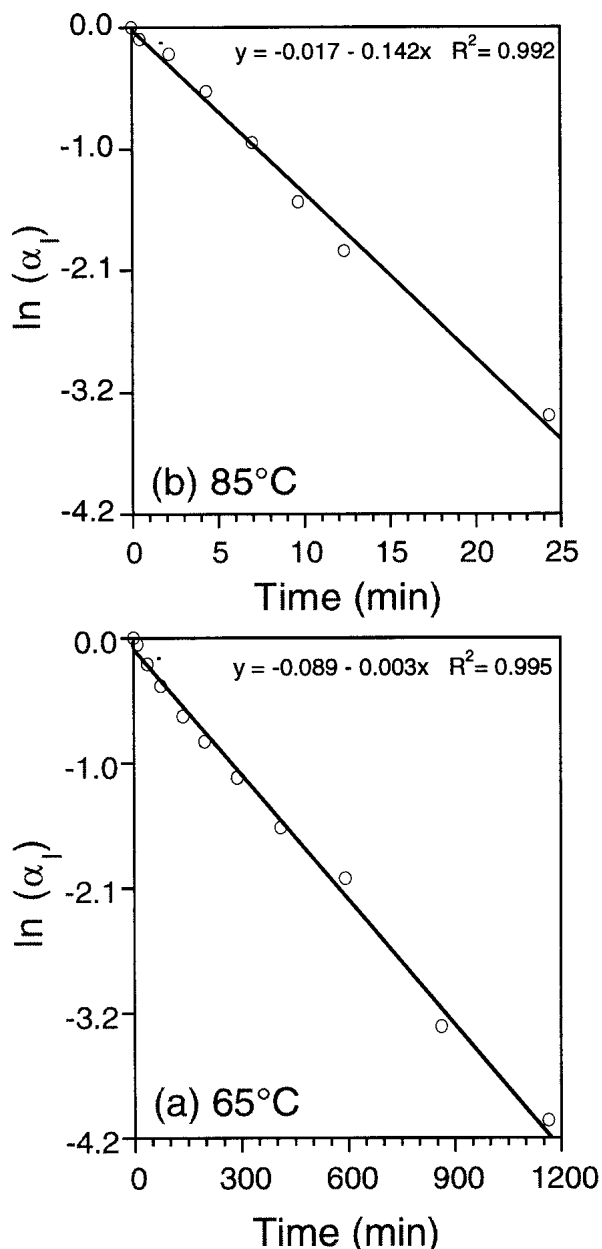


Fig. 5. First order plots of the mole fraction of aminophylline monohydrate remaining as a function of time, at (a) 65°C, and at (b) 85°C.

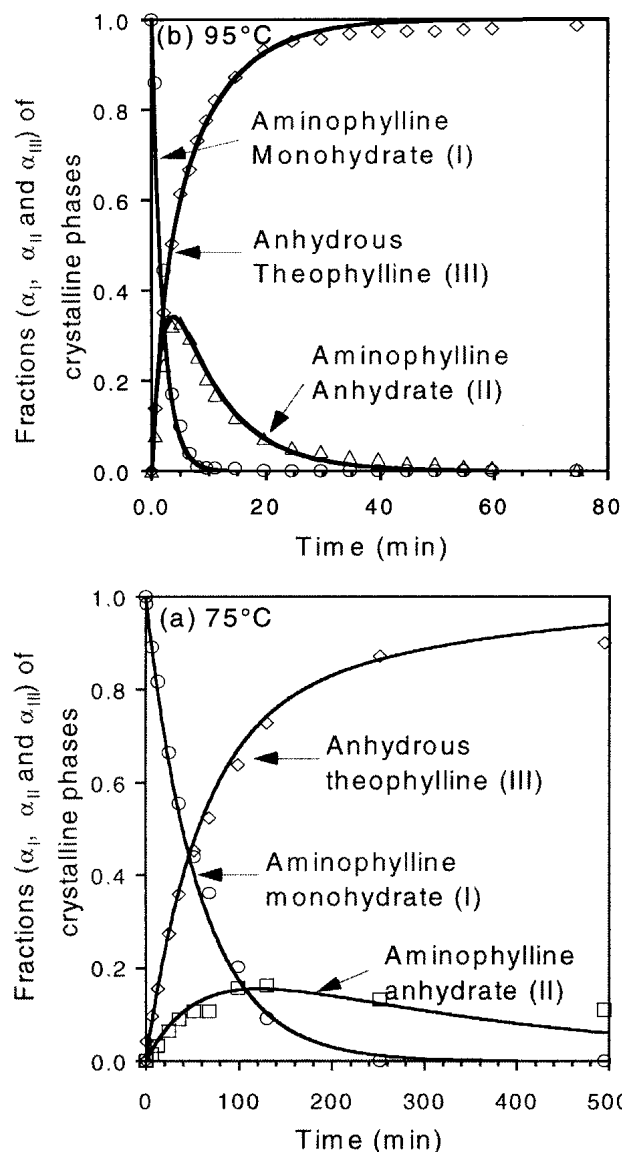


Fig. 6. Plot of the mole fractions of the reactant (aminophylline monohydrate, α_I), intermediate (aminophylline anhydrate, α_{II}), and product (theophylline, α_{III}) as a function of time at (a) 75°C and at (b) 95°C. The solid lines were generated using the proposed model (Equations 8 and 10), while the data points were experimentally obtained.

ences could be attributed to the fact that k_1 has a more pronounced temperature dependence than k_2 and k_3 .

Finally, the values of k_1 , k_2 and k_3 obtained above were used to generate theoretical isothermal TGA curves (Fig. 8). These were compared to the experimentally obtained isothermal TGA curves. In general, there is a very good agreement between the two. Small differences may be attributed to the difference in sample packing and geometry. As expected, the proposed model overestimates the weight loss at later time points. This again suggests the formation of product layer at the surface, which slows down the removal of gaseous products. It is clear that the TGA curves alone would provide little information on the kinetics or mechanism of this complex reaction. Thus, this work demonstrates that isothermal XRD can be a necessary tool in the investigation of complex reactions with overlapping reaction steps.

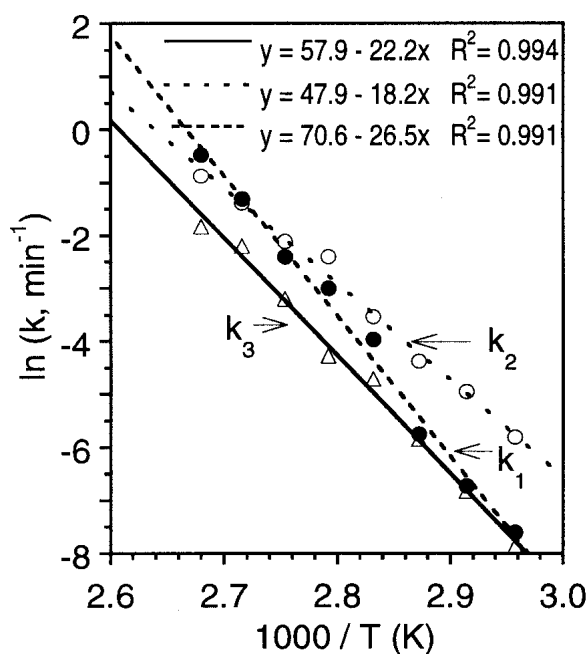


Fig. 7. Arrhenius plots for the three reaction steps (see Scheme 1) in the decomposition of aminophylline monohydrate (I).

The plots in Fig. 7 can be extrapolated to obtain the rate constants k_1 , k_2 and k_3 at room temperature. Thus, the decomposition kinetics at room temperature can be predicted. This is potentially important information, useful for predict-

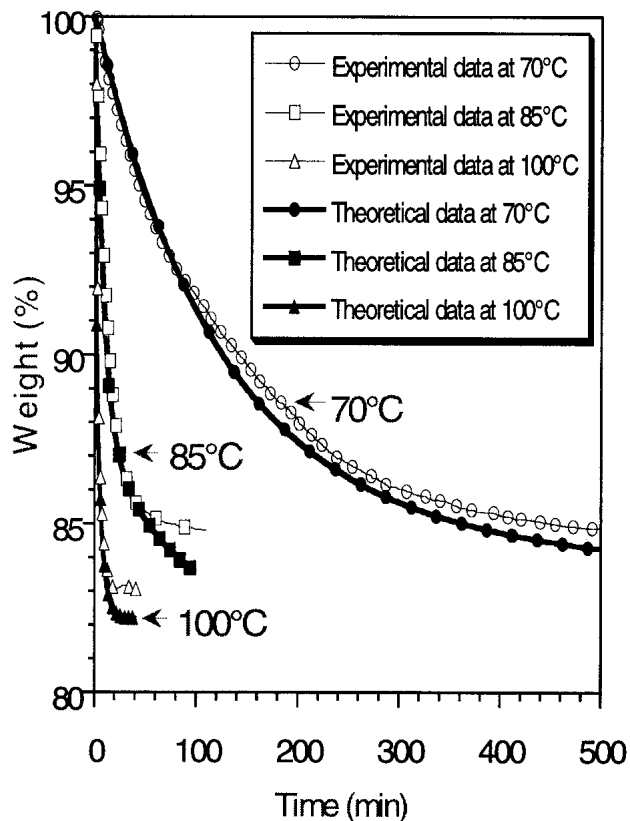


Fig. 8. Comparison of the experimentally obtained TGA curves with those generated "theoretically." The theoretical plots were generated using the rate constants obtained from the XRD experiments.

ing the shelf-life of pharmaceutical products. The extrapolated values of k_1 , k_2 and k_3 at room temperature (22°C) were 5.2×10^{-9} , 1.2×10^{-6} , and $3.0 \times 10^{-8} \text{ min}^{-1}$ respectively, whereas at 5°C (assumed as the refrigerator temperature), these values were 2.2×10^{-11} , 2.9×10^{-8} , and $3.1 \times 10^{-10} \text{ min}^{-1}$ respectively. At both the temperatures, the value of k_2 is about three orders of magnitude higher than that of k_1 . As a result, at lower temperatures, the reaction will proceed predominantly through the route **I** → **III** and not through **I** → **II** → **III**. Hence, there should be no appreciable build up of **II** during decomposition and the reaction can be approximated to be consisting of a single step: **I** → **III**. This was indeed the case when aminophylline was stored at room temperature for a few months. Based on the extrapolated values of the rate constants, the estimated time required for decomposition of 10% of **I** was about 2 months. This is unacceptable for a solid formulation of aminophylline. However, at 5°C, the estimated decomposition was only about 3% in 2 years.

Since the extrapolation has been carried out over a wide temperature range, the results should be viewed with caution. The reaction mechanism, over the temperature range of 60 to 100°C, may be different from that at lower temperatures. The water vapor pressure is expected to significantly influence the dehydration kinetics. In such situations, the extrapolation may not be valid. Moreover, in formulations, the effect of excipients will need to be considered. Interestingly, the assay method described in the USP monograph of aminophylline cannot distinguish between aminophylline and theophylline (28).

The Arrhenius plots thus enabled some physically-relevant interpretation of the kinetic data. It is evident that the preferred reaction pathway, at low temperatures, is the simultaneous loss of water and ethylenediamine (k_2). The high activation energy for the dehydration reaction (k_1) makes this pathway secondary at temperatures of practical interest (at and around ambient temperature). Under such conditions, it is easier to cause the simultaneous loss of water and ethylenediamine than just the dehydration process.

Errors in Quantitative XRD

The nature of the work necessitated a careful consideration of the sources of error in quantitative XRD.

Preferred Orientation

Microscopic examination revealed that the sample ("as is" **I**) consisted of irregularly shaped particles (10 to 100 μm) with no pronounced habit. Therefore errors due to preferred orientation are unlikely to be significant. In order to confirm that the orientation of the individual particles in the powder bed does not change during the decomposition, the sample was subjected to hot-stage microscopy. When **I** was heated at 10°C/min, the size and shape of the individual particles did not change from room temperature to 200°C. Thus, the habit appears to be unaffected throughout the reaction. Therefore, the orientation of the particles should remain unchanged during the entire experiment. This was supported by the observation that there was no perceptible change in the bulk volume of the powder during the isothermal XRD experiments. Therefore the sample and the holder surfaces were coplanar throughout the reaction. The other sources of error were also

taken into consideration during the experimental design, data collection and data analysis (10).

CONCLUSIONS

Variable temperature XRD was used to study the kinetics of decomposition of aminophylline monohydrate. Since the reactant, intermediate and the product were all crystalline, it was not only possible to identify the intermediate formed but also to simultaneously quantify aminophylline monohydrate (reactant; **I**), aminophylline anhydrate (intermediate; **II**) and anhydrous theophylline (product; **III**) as a function of time. The XRD technique not only revealed the multiple pathways of decomposition, but also permitted calculation of the relevant rate constants. All the three reaction steps followed first-order kinetics. The rate constants k_1 (**I** to **II**), k_2 (**I** to **III**) and k_3 (**II** to **III**) were determined as a function of temperature. The activation energies were determined and the temperature dependence of k_1 was more pronounced than that of k_2 and k_3 . Isothermal TGA, which finds widespread use to study such reactions was deemed unsuitable to study the decomposition of **I**, since there were overlapping thermal events. However, it was possible to use TGA as a supplementary technique.

ACKNOWLEDGMENTS

The helpful comments of Dr. Raymond Skwierczynski (3M Pharmaceuticals, St. Paul, MN) and an anonymous reviewer are gratefully acknowledged.

REFERENCES

1. J. Halebian and W. McCrone. Pharmaceutical applications of polymorphism. *J. Pharm. Sci.* **58**:911–929 (1969).
2. D. C. Monkhouse and L. van Campen. Solid state reactions—theoretical and experimental aspects. *Drug Dev. Ind. Pharm.* **10**: 1175–1276 (1984).
3. H. G. Brittain. *Overview of Physical Characterization Methodology*. In H. G. Brittain (ed.), *Physical Characterization of Pharmaceutical Solids*, Marcel Dekker, Inc., New York, 1995, pp. 1–35.
4. S. Byrn, R. Pfeiffer, M. Ganey, C. Hoiberg, and G. Poochikian. Pharmaceutical solids: a strategic approach to regulatory considerations. *Pharm. Res.* **12**:945–954 (1995).
5. N. V. Phadnis and R. Suryanarayanan. Polymorphism in anhydrous theophylline—implications on the dissolution rate of theophylline tablets. *J. Pharm. Sci.* **86**:1256–1263 (1997).
6. H. G. Brittain. *Polymorphism in Pharmaceutical Solids*, Marcel Dekker, New York, 1999.
7. S. R. Byrn, R. R. Pfeiffer, and J. G. Stowell. *Solid State Chemistry of Drugs*, 2nd edition, SSCI, West Lafayette, Indiana, 1999.
8. K. A. Connors, G. L. Amidon, and V. J. Stella. *Chemical Stability of Pharmaceuticals: a Handbook for Pharmacists*, Wiley, New York, 1986.
9. J. Han and R. Suryanarayanan. Influence of environmental conditions on the kinetics and mechanism of dehydration of carbamazepine dihydrate. *Pharm. Dev. Tech.* **3**:587–596 (1998).
10. R. Suryanarayanan. *X-ray powder diffractometry*. In H. G. Brittain (ed.), *Physical Characterization of Pharmaceutical Solids*, Marcel Dekker, New York, 1995, pp. 187–223.
11. S. K. Rastogi and R. Suryanarayanan. *Characterization of Delivery Systems, X-ray Powder Diffraction*. In E. Mathiowitz (ed.), *Encyclopedia of Controlled Release*, John Wiley and Sons, New York, 1999, pp. 275–285.
12. S. P. Duddu, A. Khin-Khin, D. J. W. Grant, and R. Suryanarayanan. A novel X-ray powder diffractometric method for studying the reaction between pseudoephedrine enantiomers. *J. Pharm. Sci.* **86**:340–345 (1997).

13. E. Shefter, H. L. Fung, and O. Mok. Dehydration of crystalline theophylline monohydrate and ampicillin trihydrate. *J. Pharm. Sci.* **62**:791–794 (1973).
14. Y. Li, J. Han, G. G. Z. Zhang, D. J. W. Grant, and R. Suryanarayanan. *In situ* dehydration of carbamazepine dihydrate—a novel technique to prepare amorphous anhydrous carbamazepine. *Pharm. Dev. Tech.* **5**:257–266 (2000).
15. J. Han and R. Suryanarayanan. A method for the rapid evaluation of the physical stability of pharmaceutical hydrates. *Thermochim. Acta* **329**:163–170 (1999).
16. H. Hashizume, S. Shimomura, H. Yamada, T. Fujita, and H. Nakazawa. An X-ray diffraction system with controlled relative humidity and temperature. *Powder Diffr.* **11**:288–289 (1996).
17. R. A. Kuhnel and S. J. van der Gaast. Humidity controlled diffractometry and its applications. *Adv. X-ray Anal.* **36**:436–449 (1993).
18. S. K. Rastogi, M. Zakrzewski, and R. Suryanarayanan. Investigation of solid-state reactions in pharmaceutical systems using variable temperature X-ray powder diffractometry. I. Aspartame hemihydrate. *Pharm. Res.* **18**:267–273 (2001).
19. K. D. Thakker and L. T. Grady. *Aminophylline*. In K. Florey (ed.), *Analytical Profiles of Drug Substances*, Academic Press, New York, 1982, pp. 1–44.
20. Y. Kawashima, S. Aoki, H. Takenaka, and Y. Miyake. Preparation of spherically agglomerated crystals of aminophylline. *J. Pharm. Sci.* **73**:1407–1410 (1984).
21. J. Nishijo and F. Takenaka. Studies of the properties of the complex medicines. I. Differential thermogravimetric analysis of Aminophylline. *J. Pharm. Soc. Jap.* **99**:824–829 (1979).
22. Y. Ishiguro, M. Sawada, K. Ohmayu, and K. Kawabe. On the volatility of ethylenediamine from aminophylline. *J. Pharm. Soc. Jap.* **102**:211–214 (1982).
23. P. L. Klug and L. E. Alexander. *X-ray Diffraction Procedures for Polycrystalline and Amorphous Materials*, Wiley, New York, 1974.
24. Powder Diffraction File (PDF-2), International Centre for Diffraction Data, Newtown Square, Pennsylvania, 1996.
25. J. T. Carstensen. Stability of solids and solid dosage forms. *J. Pharm. Sci.* **63**:1–14 (1974).
26. E. Y. Shalaev, M. Shalaeva, S. R. Byrn, and G. Zografi. Effects of processing on the solid-state methyl transfer of tetraglycine methyl ester. *Int. J. Pharm.* **152**:75–88 (1997).
27. H. Schmalzreid. *Chemical Kinetics of Solids*, VCH Verlagsgesellschaft mbH, Weinheim, Germany, 1995.
28. The United States Pharmacopeia/The National Formulary, 24th revision, United States Pharmacopeial Convention, Rockville, MD, 1999, p. 115.